Biochimica et Biophysica Acta 1818 (2012) 537–550

Contents lists available at SciVerse ScienceDirect

Biochimica et Biophysica Acta

journal homepage: www.elsevier.com/locate/bbamem

Probing molecular interactions of poly(styrene-*co*-maleic acid) with lipid matrix models to interpret the therapeutic potential of the co-polymer

Shubhadeep Banerjee [a,b], Tapan K. Pal [b], Sujoy K. Guha [a,*]

[a] School of Medical Science and Technology, Indian Institute of Technology, Kharagpur 721302, India
[b] Bioequivalence Study Centre, Department of Pharmaceutical Technology, Jadavpur University, Kolkata 700032, India

ARTICLE INFO

Article history:
Received 1 August 2011
Received in revised form 18 November 2011
Accepted 8 December 2011
Available online 14 December 2011

Keywords:
Poly(styrene-*co*-maleic acid)
Liposome
ATR-FTIR
DSC
NMR

ABSTRACT

To understand and maximize the therapeutic potential of poly(styrene-*co*-maleic acid) (SMA), a synthetic, pharmacologically-active co-polymer, its effect on conformation, phase behavior and stability of lipid matrix models of cell membranes were investigated. The modes of interaction between SMA and lipid molecules were also studied. While, attenuated total reflection-Fourier-transform infrared (ATR-FTIR) and static ^{31}P nuclear magnetic resonance (NMR) experiments detected SMA-induced conformational changes in the headgroup region, differential scanning calorimetry (DSC) studies revealed thermotropic phase behavior changes of the membranes. ^{1}H NMR results indicated weak immobilization of SMA within the bilayers. Molecular interpretation of the results indicated the role of hydrogen-bond formation and hydrophobic forces between SMA and zwitterionic phospholipid bilayers. The extent of membrane fluidization and generation of isotropic phases were affected by the surface charge of the liposomes, and hence suggested the role of electrostatic interactions between SMA and charged lipid headgroups. SMA was thus found to directly affect the structural integrity of model membranes.

1. Introduction

Synthetic polymers are currently generating increased interest as therapeutic agents owing to their enhanced pharmacokinetic profiles, improved efficacy and better physicochemical stability relative to small molecule drugs. The high-molecular weight nature coupled with the opportunity for polyvalent binding interactions has made polymers interesting candidates for novel chemical entities for therapeutic applications in which low-molecular weight drugs have either failed or exhibited inadequate benefits [1]. Though these polymers are presently being extensively used in the formulation of small molecule drugs, primarily as carriers or sustained release devices, they can also be used as therapeutics on their own [2].

Poly(styrene-*co*-maleic acid) (SMA) is a synthetic co-polymer with attractive chemical [3] and biological properties. The potential of SMA as a polymeric drug has already been exploited with the clinical success of SMANCS, a conjugate of immunostimulatory styrene maleic acid co-polymer with the potent yet toxic anti-tumor polypeptide neocarzinostatin (NCS), in liver and lung cancer [4–6]. Recent revelation of the potential of SMA and its derivatives in effectively inhibiting human immunodeficiency virus type 1 (HIV-1) [7,8], by preventing virus adsorption on the surface of target cell membranes, has generated considerable interest.

SMA co-polymers have also been reported to be strong inhibitors of spermatozoa motility [9]. The spermicidal activity of the co-polymer has been attributed to the presence of carboxylic groups, which induces a low-pH environment responsible for killing spermatozoa.

Our laboratory has been actively involved in researching the therapeutic applicability of styrene maleic acid/anhydride co-polymers in human sexually transmitted disease prevention and fertility control, with a special attention toward genital HIV-1 infections [10]. A new male non-hormonal contraceptive RISUG (an acronym for Reversible Inhibition of Sperm Under Guidance), with styrene maleic acid/anhydride co-polymers as active pharmaceutical ingredients, has emerged from our laboratory and is currently undergoing extended Phase III clinical trials throughout India.

The activity of the pharmacologically-active styrene maleic acid co-polymer for the treatment of a wide spectrum of human diseases is noteworthy. However, to utilize the therapeutic potential of this co-polymer to the fullest, a detailed understanding of the mechanism by which SMA molecules interact with cell membranes at the molecular level is of critical importance, especially when one considers the efficacy and safety of the polymer therapeutic, since interaction with exogenous amphiphilic SMA can directly affect the structural integrity of the cell [11]. It has already been reported that the hydrophobic regions of SMA play an important role in the penetration of the lipid bilayer of cell membranes, and the anionic portion of the co-polymer facilitates the internalization and binding of the drug-polymer conjugate with the hydrophobic milieu of the cell [12]. SMA is also known to induce surface charge imbalance on human spermatozoa membrane, which leads to the release of acrosomal enzymes hyaluronidase and acrosin. This

* Corresponding author. Tel.: +91 3222 283574; fax: +91 3222 282221.
E-mail address: guha_sk@yahoo.com (S.K. Guha).

0005-2736/$ – see front matter © 2011 Elsevier B.V. All rights reserved.
doi:10.1016/j.bbamem.2011.12.010

ultimately leads to spermatozoa damage [13,14]. It therefore becomes imperative to elucidate the influence of SMA on lipid matrix models of cell membranes in order to improve the therapeutic potential of the co-polymer by enhancing biological activity and diminishing side effects.

This study aims to characterize the conformational changes in the SMA-doped liposomes and dry lipid/co-polymer films, detect the changes induced by the co-polymer on the phase behavior and stability of model membranes and discern the nature of intermolecular interactions at work between SMA and lipid molecules.

We have investigated the interactions of SMA with different sets of dry lipid films and multilamellar vesicles, composed of zwitterionic phospholipid distearoylphosphatidylcholine with cholesterol and charged lipids added to it, to mimic various types of cell membranes differing in composition and surface charge. ATR-FTIR studies were performed to detect the conformational changes induced by the co-polymer in the lipid acyl chain region as well as in the headgroup and interfacial regions of the lipid molecules. DSC, a thermal analytical technique, was used to study the thermotropic phase behavior of liposomes from which the molecular interactions between the co-polymer and phospholipids were quantitatively probed. ^{31}P NMR experiments were carried out to characterize the effect of the co-polymer on the structure and dynamics of multilamellar vesicles and to get a more direct indication of the effects induced by SMA in the headgroup region of the vesicles. Proton NMR spectroscopy was used to probe the existence and nature of interactions between the amphiphilic co-polymer and phospholipid molecules.

2. Materials and methods

2.1. Materials

1,2-distearoyl-sn-glycero-3-phosphocholine (DSPC), dimethyldioctadecylammonium bromide (DODAB), dicetylphosphate (DCP) and cholesterol (CHOL) (Fig. 1A–D) were purchased from Sigma Chemicals Co., USA. 4-2-hydroxyethyl-1-piperazineethanesulfonic acid (HEPES) was obtained from Sisco Research Laboratories Pvt. Ltd., India. Deuterium oxide (D_2O) and deuterated methanol (CD_3OD) were bought from Cambridge Isotope Laboratories Inc., USA. HPLC grade chloroform and methanol and analytical grade sodium chloride were purchased from Merck, India. All chemicals were used as obtained without further purification. Milli-Q water obtained from Milli-Q Integral 3 system (Millipore, France) was used for all experiments.

2.2. Methods

2.2.1. Synthesis of poly(styrene-co-maleic acid)

Styrene maleic acid co-polymer (Fig. 1E) was prepared according to the method described in the United States patent number 5488075 [15]. Briefly, maleic anhydride (MAn) and styrene (St) monomers in 1:1 (w/v) ratio were taken in glass bottles to which ethyl acetate was added and dry nitrogen gas purged. Polymerization was achieved by gamma irradiation at 37 °C, using a dose rate of 0.3 Gy/s and a total dosage of 2.4 Gy. The co-polymer was precipitated with petroleum ether and soxhlet distilled using 1,2-dichloro ethane and Milli-Q water respectively. Styrene maleic anhydride co-polymer obtained after careful purification from unreacted monomers was subjected to base catalyzed hydrolysis by refluxing with sodium hydroxide solution. The co-polymer was then recovered by acid precipitation using hydrochloric acid. The obtained SMA was washed several times with acidified Milli-Q water to remove any sodium salts present and then dried and used for further experiments. The weight-average molecular weight (M_w = 850,000 Da) of the hydrolysed co-polymer was determined by gel permeation chromatography at 35 °C (Viscotek, Malvern, USA).

2.2.2. Preparation of multilamellar vesicles (MLVs)

Multilamellar vesicles were prepared according to the lipid film hydration method [16] with slight modifications. Briefly, required

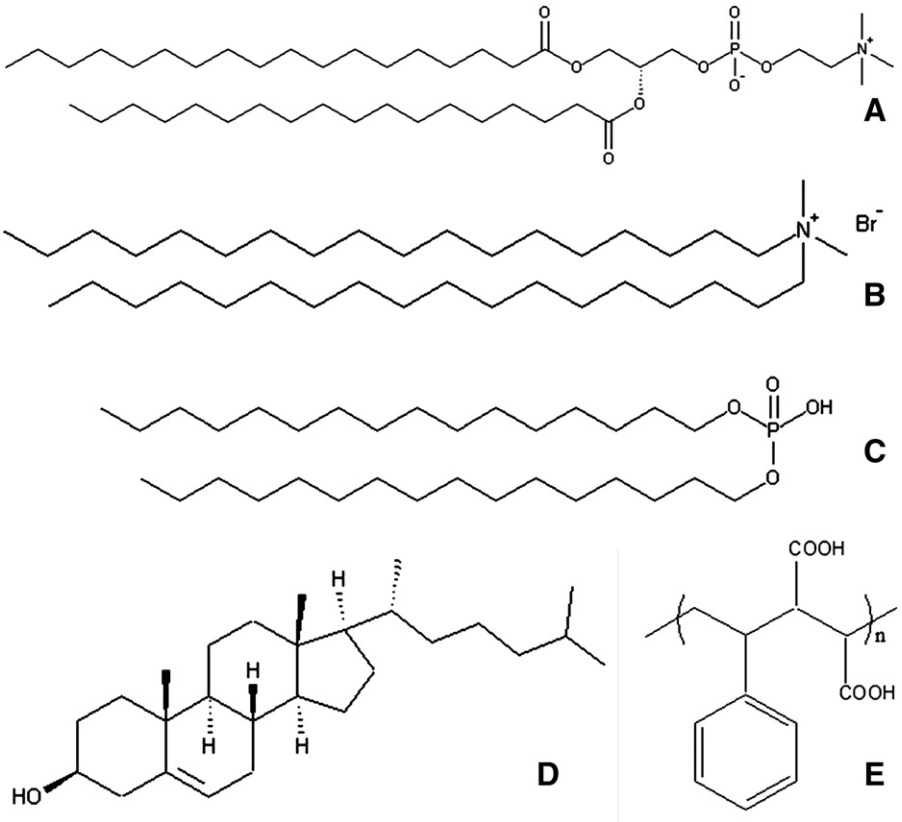

Fig. 1. Chemical structures of A, 1, 2-distearoyl-sn-glycero-3-phosphocholine (DSPC); B, dimethyldioctadecylammonium bromide (DODAB); C, dicetylphosphate (DCP); D, cholesterol (CHOL) and E, styrene maleic acid (SMA) co-polymer.

amounts of DSPC, cholesterol and charged lipids were dissolved in methanol/chloroform mixture (1:1 v/v) in round-bottom flasks to produce final molar ratios of 7:1 (DSPC:CHOL) or 7:2:1 (DSPC: DODAB/DCP:CHOL) respectively. Appropriate volume of the stock solution of SMA (in methanol) was added to it and vortexed to form a homogeneous solution. The phospholipid to co-polymer molar ratio of 100:1 was maintained for all the systems. The organic solvents were evaporated in a rotavapor (R210, Büchii Switzerland) attached with a vacuum controller to form lipid and lipid/co-polymer thin films along the inside wall of the flasks. The round-bottom flasks were then attached to high vacuum for 6 h to remove any traces of organic solvents left behind. The dried films were hydrated with an appropriate volume of filtered hepes buffered saline (10 mM hepes and 150 mM NaCl, pH 7.0) and incubated at 65 °C (~10 °C above the phase transition temperature of the phospholipid) by rotating the flasks in the rotary evaporator without vacuum for 1 h along with intermittent severe vortexing to remove the entire film from the wall of the flasks and form homogeneous suspensions. The obtained multilamellar vesicles (MLVs) were then subjected to five freeze-thaw cycles by alternatively freezing in liquid nitrogen and then thawing it at 65 °C in a water bath. The resulting liposomes were used in subsequent experiments. All experiments were performed with freshly prepared liposomes. For NMR experiments, all sets of MLVs were suspended in hepes buffered saline made in D_2O (pD 7.0) and had a lipid concentration of 40 mg/ml. For all other experiments, liposome suspensions were prepared with lipid concentrations maintained at 20 mg/ml and were diluted according to the requirement of respective experiments.

2.2.3. Attenuated total reflection-Fourier-transform infrared (ATR-FTIR) spectroscopy

Dry lipid and lipid/co-polymer films having the same molar ratios as mentioned in Section 2.2.2 were prepared by spreading 200 μl of methanol/chloroform (1:1, v/v) solution of lipid and lipid/co-polymer mixtures on one surface of zinc selenide (ZnSe) ATR crystal and then evaporating the solvent under a stream of dry nitrogen gas. The concentration of lipids in chloroform/methanol solution was 10 mg/ml. The experiments were carried out in Nexus-870 FTIR spectrometer (Thermo Nicolet Corporation, USA). A total of 100 scans were collected and co-added with a spectral resolution of 2 cm^{-1}. The data obtained was analyzed using the OMNIC software (version 6.0 A) supplied with the instrument. All spectra reported in this study were obtained after subtraction of the background spectra measured with the blank ZnSe crystal.

2.2.4. Particle size and zeta potential measurements

MLV suspensions were adequately diluted with filtered hepes buffered saline (HBS, pH 7.0), and their size and zeta potential values were measured in triplicate on a Zetasizer NanoZS instrument (Malvern, U.K.) equipped with a 4 mW He–Ne laser (λ = 633 nm) at 25 °C. The data obtained was analyzed using the Zetasizer 6.01 software supplied with the instrument. The zeta potential values were calculated using the Helmoholtz–Smolowkovski equation.

2.2.5. Differential scanning calorimetry (DSC)

DSC scans were performed using the high-sensitivity differential scanning calorimeter VP-DSC (MicroCal, USA). Both liposomal samples and buffer were degassed with stirring under vacuum at 23 °C for 20 min using MicroCal Thermovac, before being loaded into sample and reference cells. All thermograms were run using the same volume of buffer as reference. The samples were equilibrated at the starting temperature for 15 min prior to each scan. A scan rate of 20 °C/h was employed for the experiments which were carried out in the temperature range of 20 to 65 °C for DSPC and DSPC + CHOL samples and 20 to 80 °C for vesicles containing charged lipids, with the pressure automatically held at 25 psi for all sets. After degassing the samples, the lipid concentration was determined using a modified Bartlett phosphate assay and was found to be 6 mg/ml. Upon completion of the DSC run, the samples were checked for decomposition by thin-layer chromatography. No decomposition was observed. A baseline was run before each experiment with HBS (pH 7.0) loaded in both sample and reference cells and was subtracted from individual results on data analysis. Data were analyzed using ORIGIN software provided by MicroCal. Repeated scans for same samples were usually superimposable.

2.2.6. Nuclear magnetic resonance (NMR) spectroscopy

NMR spectra were recorded on a BRUKER AVANCE Ultra Shield™ 500 MHz spectrometer (Bruker, Switzerland). Static ^{31}P NMR experiments were carried out at 202.45 MHz with proton-decoupling during signal sampling by means of a Waltz-16 composite pulse sequence. Each spectrum was the result of accumulation of 8000 scans, sampled using 8192 complex data points. An interpulse delay of 1 s was used to improve the signal-to-noise ratio. The static ^{31}P fids were multiplied with an exponential function to increase the linewidth by 50 Hz, in order to reduce noise prior to Fourier transformation. All chemical shift values were quoted in parts per million (ppm) with reference to phosphoric acid (H_3PO_4, 0 ppm). Spectra for each sample were recorded in triplicates at temperatures ranging from 30 to 60 °C. The sample temperature was allowed to stabilize prior to acquisition and was maintained throughout the experiment. ^1H NMR experiments were carried out at 500.13 MHz with 128 transients and a relaxation delay of 1 s between transients at 30 °C. The chemical shifts for proton NMR spectra were recorded in ppm relative to tetramethylsilane (0 ppm) as internal standard. ^1H NMR experiment for SMA was performed by dissolving the co-polymer in deuterated methanol. All NMR data were processed using BRUKER TOPSPIN 2.0 software.

3. Results

3.1. ATR-FTIR spectroscopy

Phospholipids contain several IR active groups that can function as suitable spectroscopic probes of the structure and interactions in hydrophobic, interfacial and polar headgroup regions of lipid assemblies (Fig. 2, Table 1) [17].

3.1.1. Lipid hydrocarbon portion

The vibrations of the CH_2 groups are commonly used to detect hydrocarbon chain conformational disorder and mobility. The asymmetric (ν_{as}) and symmetric (ν_s) CH_2 stretch frequencies were shifted to higher frequencies in presence of SMA for DSPC, DSPC + CHOL and DSPC + CHOL + DCP systems respectively. However, for the DSPC + CHOL + DODAB system, while the ν_{as} stretch remained unaltered, the ν_s stretch was reduced in the presence of SMA. Similar set of observations were also made for the ν_{as} (CH_3) band for the different systems studied (Fig. 3). The blue shift of the maximum of ν_{as} and ν_s (CH_2), and ν_{as} (CH_3) bands indicating increased membrane fluidization was due to an increase in gauche conformer population in the lipid hydrocarbon part.

The increase in band widths observed in the case of neat and cationic dry films in presence of SMA (Fig. 3A and C), indicating alterations of lipid acyl chain dynamics, was a consequence of increased motional freedom of the methylene groups [17,18]. This result suggested SMA-induced alterations in the lateral packing of the hydrocarbon chains, which led to conformational disorder [19,20] in the DSPC and DSPC + CHOL + DODAB systems.

Further useful information regarding acyl chain packing and interchain interactions was derived from CH_2 scissoring and wagging modes. The presence of SMA had different effects on the δ_s acyl scissoring for the different systems studied. While, for the neat and cationic dry films, the peak was shifted to lower frequencies, the

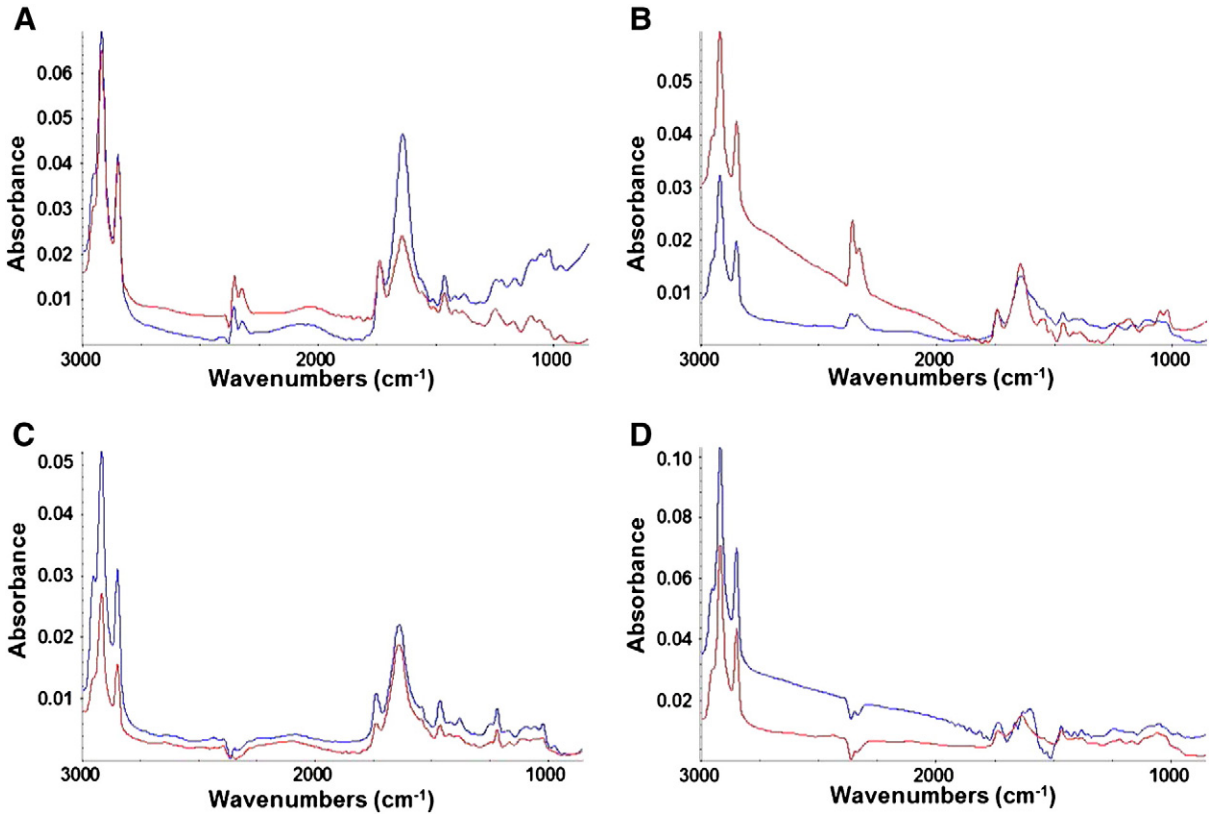

Fig. 2. ATR-FTIR spectra of A, DSPC and DSPC + SMA; B, DSPC + CHOL and DSPC + CHOL + SMA; C, DSPC + DODAB + CHOL and DSPC + DODAB + CHOL + SMA; D, DSPC + DCP + CHOL and DSPC + DCP + CHOL + SMA dry films at 25 °C in the 3000–900 cm^{-1} wavenumber region. The red and blue colors correspond to lipid and lipid/co-polymer films respectively for all the panels.

reverse was observed for the DSPC + CHOL film (Fig. 4B). However, upon incorporation of the co-polymer into DSPC + CHOL + DCP system, the broad band observed for the blank anionic dry film was split into two components (Fig. 4H). This observed spectroscopic phenomenon, defined as factor group splitting, was associated with the SMA induced arrangement of the all-trans polymethylene chains in the orthorhombic perpendicular form of subcellular packing [21].

The co-polymer induced a shift of acyl CH_2 wagging band to higher frequencies in all the systems studied. The peak originating from the terminal δ_s (CH_3) symmetric bending mode in all lipid films was also observed to be shifted by SMA. The weak band, corresponding to CH_2 scissoring adjacent to C═O group was blue shifted upon incorporation of the co-polymer. Thus, the incorporation of the co-polymer in all the cases involved a significant reorganization of the packing of the lipid hydrocarbon portion.

3.1.2. Lipid interfacial region

The polar–apolar interface in the DSPC bilayer is represented by ester carbonyl groups whose intensive ν (C═O) stretch band is composed of two components originating from two ester carbonyl groups

Table 1
Assignment of infrared absorption bands observed for different sets of dry lipid and lipid/co-polymer films.

Peak assignment system[a]	Wavenumber in cm^{-1}							
	A	B	C	D	E	F	G	H
ν_{as} (CH_3) stretch	2958	2959	2958	2959	2957	2956	2957	2958
ν_{as} (CH_2) stretch	2920	2921	2921	2922	2921	2921	2919	2920
ν_s (CH_2) stretch	2851	2852	2852	2853	2852	2851	2850	2851
ν (C═O) stretch	1738	1737	1741	1741	1739	1738	1739	1737
δ_s (CH_2) acyl scissoring	1464	1462	1463	1465	1465	1464	1465	1469 1461
δ_s (CH_2) acyl scissoring adjacent to C═O	1417	1419	1416	1415	1419	1416	n	1408
δ_s (CH_3) bend	1385	1377	1390	1381	1381	1379	1381	1379
δ_s (CH_2) acyl wagging	1311	1313	1316	1318	1317	1315	1319	b
ν_{as} (P═O) stretch	1245	1243 1217	b	1246 1219	1217	1216	1234	1237
ν_s (OC–O) stretch	1169	1163	1182	1162	1162	1168	1165	1168
ν_s (P═O) stretch	1094	1091	1092	1092	1093	1090	1091	1091
ν (R–O–P–OR′) stretch	1056	1051	b	1057	1057	1055	1050	1057
secondary C–OH (cholesterol)	–	–	1049	1046	1047	b	b	b
ν (C–OP) stretch	1019	1017	1018	1022	1023	1019	1023	1021
ν_{as} ($C-N^+-C$) stretch	968	966	n	n	n	n	n	n

[a] Compositions of the systems are as follows: A, DSPC; B, DSPC + SMA; C, DSPC + CHOL; D, DSPC + CHOL + SMA; E, DSPC + DODAB + CHOL; F, DSPC + DODAB + CHOL + SMA; G, DSPC + DCP + CHOL; H, DSPC + DCP + CHOL + SMA. Abbreviations: b, broad; n, not prominent; –, absent; s, symmetric; as, asymmetric.

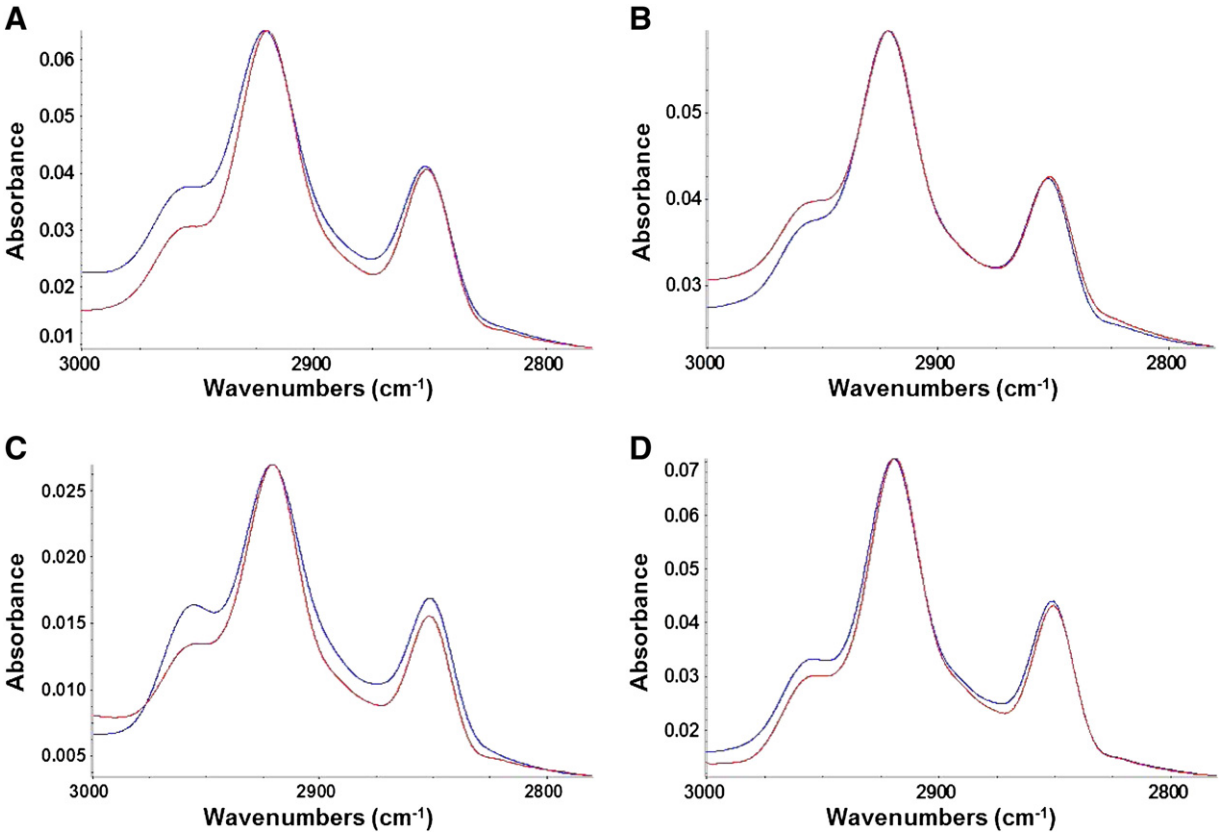

Fig. 3. Infrared spectra of acyl C – H stretching regions of DSPC and DSPC + SMA (Panel A), DSPC + CHOL and DSPC + CHOL + SMA (Panel B), DSPC + DODAB + CHOL and DSPC + DODAB + CHOL + SMA (Panel C) and DSPC + DCP + CHOL and DSPC + DCP + CHOL + SMA (Panel D) dry films at 25 °C. The red and blue colors correspond to lipid and lipid/co-polymer films respectively for all the panels.

present at the sn-1 and 2 positions in long hydrocarbon chain lipids [17]. The ATR-FTIR study of SMA-doped dry lipid films was performed to gather information about the direct interactions between the co-polymer molecules and the ester groups of phospholipids. The position of the sharp and symmetric peak of the ν (C═O) band was red shifted along with significant broadening for all the systems in presence of SMA (Fig. 4A). The observed shift of the ν (C═O) vibrations to lower frequencies was due to the hydrogen (H) bond formation between the un-ionized carboxyl groups of SMA and the phosphodiester group of lipid molecules. The role of H-bond formation was validated by the observed red shift of the ν (C═O) band after complete hydration of the dry DSPC film (data not reported). The shift toward lower frequency was due to H-bond formation between water molecules and the lipid ester groups. Moreover, in the co-polymer-loaded liposome suspensions, the water molecules were still able to form H-bonds with free ester groups unoccupied by co-polymer molecules since the ν (C═O) band was further red-shifted (data not reported) than that in the DSPC + SMA dry film with the same mole fraction of SMA and at the same temperature.

The other important feature in spectra at the interfacial region of lipid membranes is the band representative of C – O stretching, namely ν_s (OC – O) of esters of fatty acyl chains. While, the peak was observed to be red shifted in presence of SMA for DSPC and DSPC + CHOL systems, it was blue shifted for systems containing charged lipids (Fig. 4D). All, these observations not only suggested unique interactions of the co-polymer with the C═O group of the lipid molecules at the interface but also indicated compositional dependence on organizational differences of lipid molecules. Furthermore, the characteristic changes in IR behavior of CH_2 group adjacent to C═O group reported above, were in line with the changes observed for the carbonyl stretch band.

3.1.3. Lipid headgroup region

The phosphate group, characterized by two stretching vibration bands ν_{as} and ν_s (PO_2^-) respectively is sensitive to polarity changes in the headgroup region (Fig. 4C and E). The ν_{as} (PO_2^-) vibration is commonly used to detect hydrogen bond interactions between the phosphate moiety of phospholipids and proton-donor groups. The spectra displayed a notable SMA-induced red shift of ν_{as} (PO_2^-) band arising from the free phosphate groups of the lipid molecules. The small shoulder observed at lower frequency in the DSPC dry film (Fig. 4C) was due to hydrogen-bonded phosphate groups, a consequence of weak hydrogen bonding interaction between choline $N(CH_3)_3$ and phosphate groups, as reported in earlier studies [17,22,23]. SMA induced alterations in the molecular packing of the headgroup region of the phospholipid, which led to better accessibility of the proton donor groups of the co-polymer to the phosphate group of the lipid molecules [22]. This resulted in enhanced hydrogen bonding interactions between unionized carboxyl groups of SMA and phosphodiester moiety of DSPC, and ultimately caused intensification of the ν_{as} (PO_2^-) peak due to hydrogen bonded phosphate groups. The presence of the co-polymer also resulted in similar shift toward lower wavelengths for ν_s (PO_2^-) stretch bands.

The other important changes included prominent red shift of ν (R – O – P – O – R′) and C – OP stretch bands in the phosphate ester region of SMA-doped DSPC film (Fig. 4E and F). Thus, in addition to the effect on ν_{as} (PO_2^-) vibrations, concomitant changes recorded for ν (C – OP) frequencies were also in support of co-polymer-mediated changes in the phosphate group.

Further evidence of the alterations in the molecular packing of the head group region was obtained from the shift of the ν_{as} [$N(CH_3)_3$] peak (3025 cm^{-1} for neat DSPC film) to higher frequency (3029 cm^{-1}) in the presence of SMA. This was possibly due to the presence of SMA molecules between the phosphate and choline

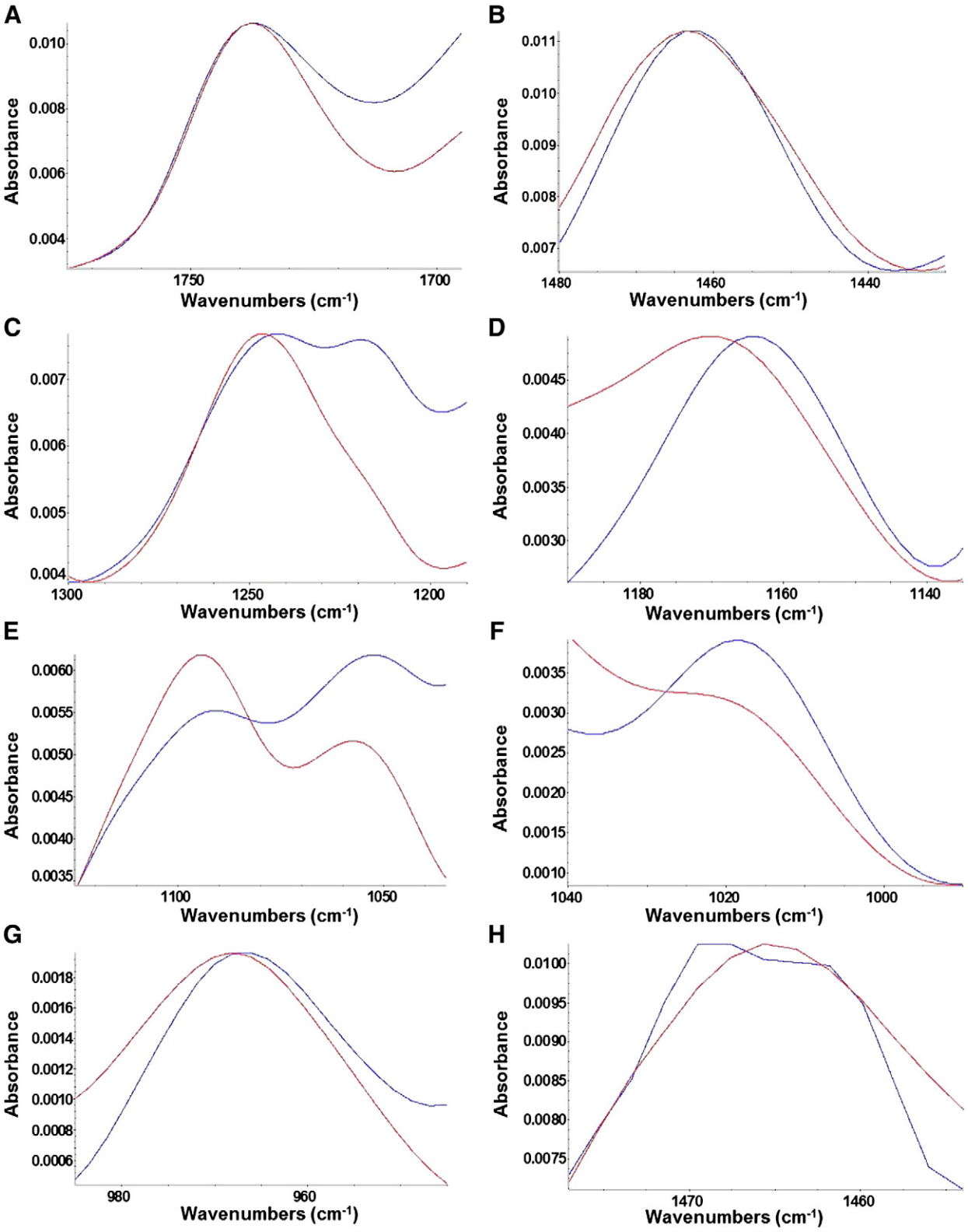

Fig. 4. Representative ATR-FTIR spectra illustrating the changes in C═0 stretch (Panel A), CH_2 acyl scissoring (Panel B), P═O asymmetric stretch (Panel C), OC – O stretch (Panel D), P═O symmetric stretch and R – O – P – OR′ stretch (Panel E), C – OP stretch (Panel F), C – N^+ – C stretch (Panel G) bands of DSPC dry films on incorporation of the co-polymer at 25 °C. Panel H depicts the changes in the contours of CH_2 acyl scissoring regions of DSPC + DCP + CHOL dry film on incorporation of SMA. The red and blue colors correspond to lipid and lipid/co-polymer films respectively for all the panels.

trimethylammonium groups, which reduced the number of CH groups influenced by PO_2^- group, and ultimately resulted in loosening of the contacts between them and distancing of the choline $N(CH_3)_3$ and phosphate groups [22,24].

3.2. Particle size and zeta potential measurements

The mean hydrodynamic diameter and zeta potential values of neat and SMA-incorporating MLVs at pH 7.0 are summarized in

Table 2. While SMA-loaded anionic MLVs displayed bimodal size distribution with a larger-size population (79%) co-existing with smaller-dimension vesicles (21%), the other MLVs exhibited unimodal symmetrical size distribution. The observed slight increase in the mean hydrodynamic diameter of the MLVs in presence of SMA was due to incorporation of the co-polymer within the bilayers [25]. However, the extent of increase varied significantly for the different sets of MLVs. This difference might probably arise due to different modes of packing of the co-polymer in different bilayers varying in composition and surface charge [26].

The presence of SMA in DSPC + CHOL + DCP MLVs resulted in the coexistence of a sizeable population of smaller-sized vesicles alongside larger MLVs. The existence of the smaller-sized vesicles might arise due to SMA-induced vesiculation of MLVs composed of anionic lipids. It has already been reported that bilayers composed of charged lipids have greater inter-lamellar spacing compared to MLVs composed of zwitterionic lipids due to inter-bilayer charge repulsion [27]. The presence of SMA within the MLVs composed of anionic lipids would further increase the charge repulsion and ultimately cause the MLVs to vesiculate in order to reduce the repulsion.

The results of the zeta potential measurements revealed significant change in the vesicle surface charge in presence of the anionic co-polymer. In fact the presence of SMA resulted in higher negative zeta potential values of the MLVs.

The interactions between polyelectrolytes and charged colloidal particles of opposite sign present rich phenomenology with several unusual colloidal properties, and are of significant interest owing to its increasing importance in different fields [28]. Interaction of anionic SMA with cationic liposomes resulted in the MLVs displaying a surface charge of opposite sign to the one that the neat liposomes originally possessed. This phenomenon referred to as 'charge inversion', occurred, when in the adsorption at the charged surface more polyions than necessary to neutralize it collapsed, and was due to strong lateral correlation among adsorbed polyelectrolytes onto oppositely charged surfaces [29].

3.3. DSC experiments

3.3.1. DSPC MLVs

The calorimetric curves of DSPC and DSPC + SMA MLVs presented a pretransition peak indicating the transformation from a tilted to rippled chain gel phase (L_{β}' to P_{β}'), a main peak (T_m) associated with the transition from a gel to a liquid crystalline phase (P_{β}' to L_{α}) due to cooperative melting of the phospholipid hydrocarbon chains, and a small shoulder next to the main peak (Fig. 5A and B). The small shoulder before the T_m referred to as 'twin peak' [30], represented a subpopulation of lipids undergoing chain melting at a lower temperature due to an induced osmotic stress across the membranes in presence of salt (in the hydrating buffer) within the vesicles. Addition of the co-polymer caused a shift of the pretransition, the main transition and the small shoulder before the main peak to lower values.

Table 2
Hydrodynamic diameter and Zeta potential values of neat and SMA-incorporating MLVs (pH7.0).

System[a]	Hydrodynamic diameter[b] (nm)	Zeta potential[b] (mV)
A	1453 ± 21.5	−3.62 ± 0.42
B	1746 ± 31.8	−8.54 ± 0.72
C	1501 ± 24.2	−4.18 ± 0.47
D	1739 ± 28.7	−8.26 ± 0.57
E	1420 ± 38.1	+12.9 ± 1.12
F	1579 ± 25.4	−8.72 ± 0.50
G	1507 ± 42.9	−17.1 ± 1.54
H	1852 ± 36.3	−26.5 ± 1.06
	194.8 ± 1.4	

[a] Compositions of the systems are as follows: A, DSPC; B, DSPC + SMA; C, DSPC + CHOL; D, DSPC + CHOL + SMA; E, DSPC + DODAB + CHOL; F, DSPC + DODAB + CHOL + SMA; G, DSPC + DCP + CHOL; H, DSPC + DCP + CHOL + SMA.
[b] Mean ± SD (n = 3).

The area under the ΔC_p versus temperature peak measures the enthalpy change (ΔH_{cal}) associated with the process [31]. The molar enthalpy of the main transition and pretransition peaks decreased on addition of SMA (Table 3). Van't Hoff enthalpy (ΔH_{vH}), a standard state quantity, is the indicator of the changes in the shape of the transition. Incorporation of the co-polymer led to the decrease of ΔH_{vH} for both the pretransition and the main transition peaks, indicating the influence of SMA on the shape of the transition [32].

The observed increase of the width at half-height ($\Delta T_{1/2}$) of the pretransition peak was due to the presence of SMA within the vesicles (Fig. 6A and B). The main transition peak was also slightly broadened with a small increase of $\Delta T_{1/2}$ along with a decrease in the peak height. The small shoulder before the main transition was, however, affected to a greater extent by the co-polymer.

The size of cooperative unit (CU) calculated from the ratio $\Delta H_{vH}/\Delta H_{cal}$, expresses the number of molecules undergoing the gel to liquid crystalline transition at the same time by forming or breaking non-covalent bonds in concert and thus, gives a measure of the cooperativity of the transition [33]. Any molecule that affects the orientation of the lipid molecules within the bilayers, influence the cooperative unit of transition. The presence of the co-polymer reduced the number of cooperative units driving the main transition, and thus indicated destabilization of the membrane. This decrease in the size of the cooperative unit was in sync with the broadening of the transition peaks reported above.

The shift of pretransition toward lower temperature and the decrease in cooperativity as observed from the broadening of the peak indicated molecular interactions between the co-polymer and zwitterionic phospholipid molecules, preferentially through hydrogen bond formation. These interactions caused perturbations and resulted in increased mobility in the polar region of the bilayers. This occurred due to the increased sensitivity of the headgroup region of the membranes to dopants in the rippled gel phase; since it is already known that the pretransition is very sensitive to the presence of foreign substances and can shift and broaden even when a very small amount of dopant is added [34,35].

The slight decrease observed for T_m, the associated broadening of the endotherm and the decrease of ΔH_{cal} and cooperative unit in presence of SMA were all indicative of the disruption of the translational order within the bilayers [36]. These changes were the result of the presence of small amount of the co-polymer, which acted as impurities in the gel phase bilayer. The decrease in the transition enthalpy was the consequence of SMA-induced diminished stability of the gel phase of the vesicles [37]. However, it should also be noted that the endotherm obtained in the presence of the co-polymer was sharp and symmetric. Thus, the decrease in ΔH_{cal} might not be associated with the intercalation of co-polymer molecules deep in the bilayer interiors.

The shift of T_m to lower temperature, resulting from the decrease of the lipid-gel phase stability, led to the preferential binding of co-polymer molecules to the fluid phase of the lipids. This indicated the importance of hydrophobic interactions of the co-polymer with the zwitterionic lipid. Furthermore, the enhanced decrease in cooperativity induced by SMA for the twin peak in comparison to the main phase transition was also noteworthy (Table 3). The decrease in cooperativity of the phase transition led to the moderate fluidization of the bilayers [38,39].

The changes observed in the DSC endotherm in presence of the co-polymer were not due to the entrapment of SMA within the aqueous chamber, as the changes detected in the thermodynamic properties were only possible by physical association of the co-polymer with lipid bilayers [33]. However, the changes observed were slightly subdued in nature because of the higher cohesion and thus lower flexibility of the di-C18 lipid acyl chains of DSPC, which have stronger

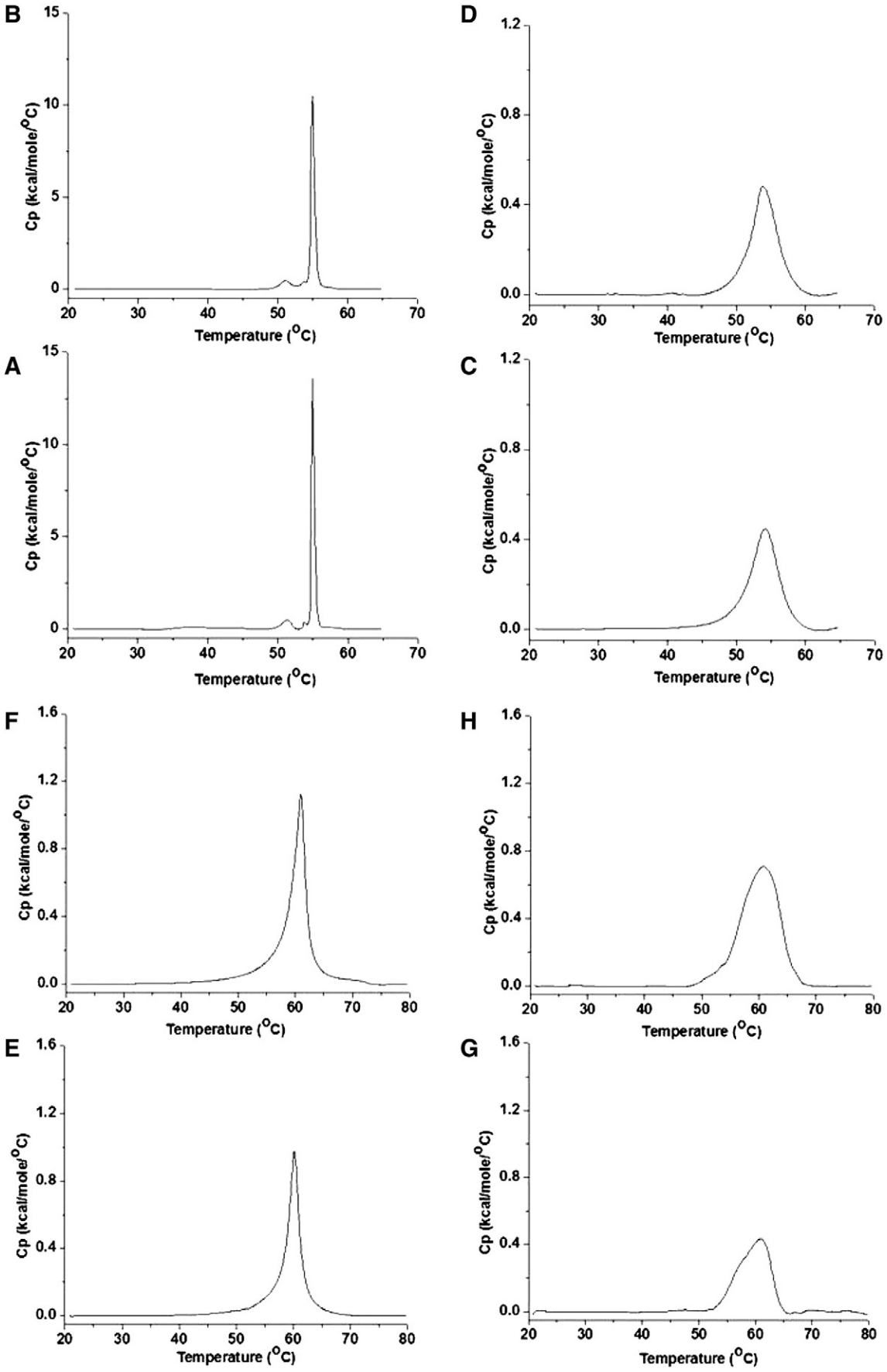

Fig. 5. Representative DSC heating scans of A, DSPC; B, DSPC + SMA; C, DSPC + CHOL; D, DSPC + CHOL + SMA; E, DSPC + DODAB + CHOL; F, DSPC + DODAB + CHOL + SMA; G, DSPC + DCP + CHOL; H, DSPC + DCP + CHOL + SMA multilamellar vesicles prepared in hepes buffered saline (10 mM Hepes + 150 mM NaCl, pH 7.0).

Table 3
Thermodynamic parameters for various MLV suspensions derived from respective calorimetric profiles.

System[a]	T_{pre}[b] (°C)	$\Delta T_{1/2}$[c], pre (°C)	ΔH_{cal}[d], pre (kcal/mol)	ΔH_{vH}[e] pre ($10^3 \times$ kcal/mol)	T_{twin}[f] (°C)	$\Delta T_{1/2}$, twin (°C)	T_m[g] (°C)	$\Delta T_{1/2}$, m (°C)	$\Delta H_{cal,\ m}$ (kcal/mol)	$\Delta H_{vH,\ m}$ ($10^3 \times$ kcal/mol)	CU[h] (no. of molecules)
A	51.41	1.2	1.50	0.37	53.75	0.63	55.01	0.45	7.63	1.49	195
B	51.13	2.2	1.22	0.34	53.70	0.90	54.95	0.53	7.1	1.24	175
C	b				–		54.12	4.50	1.95	0.16	79
D	b				–		53.91	4.22	1.89	0.17	88
E	b				–		60.19	2.41	2.78	0.27	97
F	b				–		60.99	2.85	2.40	0.22	91
G	b				–		60.71	9.33	5.1	0.08	16
H	b				–		60.31	8.60	3.81	0.11	31

[a] Compositions of the systems are as follows: A, DSPC; B, DSPC + SMA; C, DSPC + CHOL; D, DSPC + CHOL + SMA; E, DSPC + DODAB + CHOL; F, DSPC + DODAB + CHOL + SMA; G, DSPC + DCP + CHOL; H, DSPC + DCP + CHOL + SMA.
[b] T_{pre} = pretransition temperature.
[c] $\Delta T_{1/2}$ = temperature width at half peak height.
[d] ΔH_{cal} = enthalpy change.
[e] ΔH_{vH} = van't Hoff enthalpy change.
[f] T_{twin} = temperature of the twin peak.
[g] T_m = transition temperature.
[h] CU = size of cooperative unit.

hydrophobic chain interactions that caused the bilayers to be less perturbed [40,41].

The endotherms obtained were symmetric in nature, which indicated ideal mixing and absence of any lateral heterogeneity. This was the result of freeze-thawing, which improved the penetration of exogenous SMA molecules throughout MLVs due to transient damage to the bilayers, a consequence of ice crystal formation [42,43]. This led to uniform distribution of the co-polymer molecules within the bilayers and reduction of the percentage of aggregated co-polymers [34].

3.3.2. DSPC + CHOL MLVs

Eukaryotic membranes usually contain a certain fraction of cholesterol, which has several different functions in cells; one of its primary roles being in the modulation of the physical properties of the plasma membrane phospholipid bilayer [44]. Hence, it is of significance to use phospholipid–cholesterol mixtures in addition to pure phospholipids to model eukaryotic membranes in a more realistic manner [37]. However, it has already been reported that the addition of cholesterol to phospholipid bilayers significantly broadens the lipid phase transition in DSC measurements, and ultimately abolishes the main phase transition above 20–25 mol% cholesterol [45]. Addition of 12.5 mol% of cholesterol, which provided relatively high cholesterol content in the phospholipid bilayers [37], led to the complete abolition of the pretransition of the vesicles, and the main phase transition endotherm was downshifted (Fig. 5C) along with significant decrease in cooperativity and the phase transition enthalpy. The main transition was comprised of superimposed lower-temperature sharp and higher-temperature broad components as reported earlier [37,44], with the former being the major component. The sharp component was assigned to the melting of cholesterol-poor domains and the broad component to the melting of cholesterol-rich domains.

Incorporation of the co-polymer to the DSPC + CHOL binary mixture led to the shift of the main transition to lower temperature (Fig. 5D) and was associated with an increased cooperativity and cooperative units and negligibly reduced molar enthalpy (Table 3). The changes observed in the thermogram might be due to the formation of cholesterol enriched domains in the binary phospholipid–cholesterol mixtures, a consequence of increased DSPC-cholesterol demixing in presence of SMA [37].

3.3.3. DSPC + CHOL + DODAB/DCP MLVs

Prokaryotic cellular membranes consist of abundant anionic phospholipids, which are responsible for their negative charge [37]. It is also known that epididymal maturation induces a significant increase in the negative charge of the human spermatozoa membrane due to the uptake of anionic lipids [46]. The zeta potential of Y and X-chromosome bearing human sperms has been reported to be approximately −16 and −20 mV respectively [47]. Hence, the presence of charged lipids plays an important role in the interaction of drugs with cellular membranes. Addition of 20 mol% of anionic lipid into DSPC + CHOL binary mixture in the present study generated adequate surface charge to efficiently mimic human spermatozoa membrane which also has a significant amount of anionic lipids in addition to cholesterol and zwitterionic phospholipids [48]. Incorporation of equivalent amount of cationic lipid generated significant positive charge on the membrane surface to render them suitable for studying the interactions of anionic SMA with model cationic membrane systems.

Incorporation of both cationic and anionic lipids to the DSPC + CHOL binary mixture led to the upshift of the T_m. While, the incorporation of the cationic lipid led to increased cooperativity with significant narrowing of the endotherm (Fig. 5E), significant broadening and decreased cooperativity of the main transition peak was observed in presence of anionic lipid (Fig. 5G). Lateral heterogeneity induced by anionic lipid indicated low miscibility of the lipid mixture and ultimately resulted in phase separation. The presence of lamellar phase for anionic lipid assembly was substantiated by the cooperativity unit which, though drastically reduced, was well above unity, unlike micelles [49].

While, the incorporation of SMA into charged lipid mixtures showed an upshift of T_m for cationic vesicles (Fig. 5F), a downshift was observed in the case of anionic vesicles (Fig. 5H). In contrary to the decreased cooperativity and cooperative units observed for cationic vesicles, the presence of the co-polymer led to an increased cooperativity and cooperative units along with the removal of lateral heterogeneity in anionic vesicles.

The observed SMA-induced upshift of T_m in cationic vesicles was due to electrostatic attraction between the anionic co-polymer and the positively charged lipid molecules, which led to the restriction of the mobility of lipid acyl chains and thereby increased the thermal energy requirement for lipid chain expansion [32], [50]. However, the electrostatic repulsion between the co-polymer and negatively charged lipids in the anionic vesicles led to weakened interaction and thus resulted in fluidization of the bilayer [51].

3.4. NMR spectroscopy

3.4.1. ^{31}P NMR spectroscopy results

The changes in the co-polymer-induced phospholipid phase behavior were observed from the alterations in the characteristic

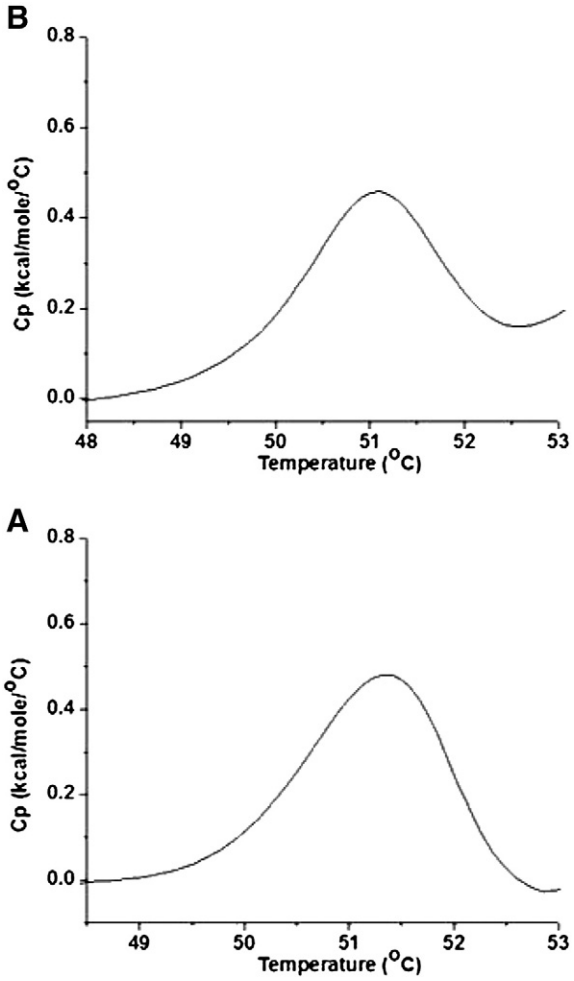

Fig. 6. Enlarged view of the pretransition region of the thermograms of A, DSPC and B, DSPC + SMA MLVs.

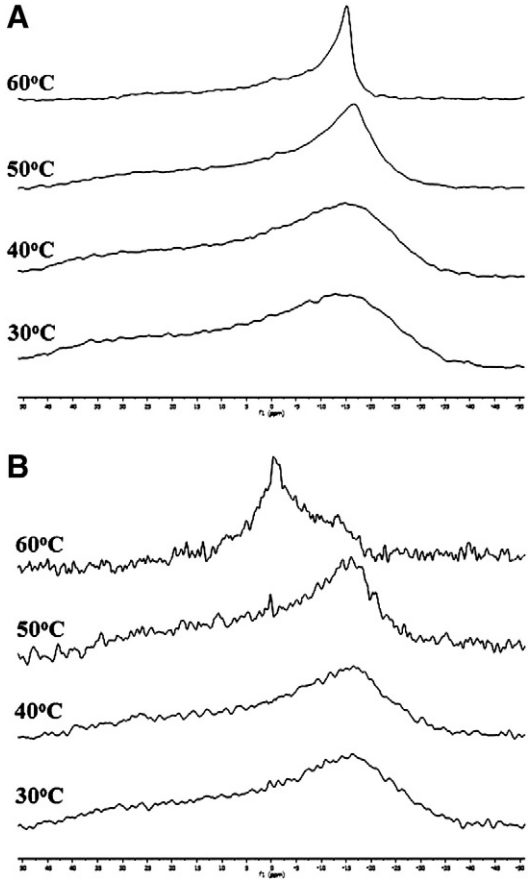

Fig. 7. 202.45 MHz ^{31}P NMR spectra of DSPC (Panel A) and DSPC + SMA (Panel B) MLVs as a function of temperature at a fixed phospholipid:co-polymer molar ratio of 100:1.

intensity distribution of the chemical shift anisotropy (of the phosphate group) dominated line shapes of wide line ^{31}P NMR spectroscopy [52]. The line shape of the ^{31}P NMR signal strongly depends on the conformation, orientation and dynamics of the phosphodiester moiety of phospholipid molecules and was thus, used to study the changes in the polymorphic phase behavior of the membranes in presence of SMA [17].

3.4.1.1. DSPC MLVs. Randomly oriented DSPC and DSPC + SMA MLVs in the gel phase (30 °C) exhibited characteristic asymmetric line shape with a high field peak and a low field shoulder arising from the perpendicular and parallel alignment of the long axis of the lipid molecules to the direction of the magnetic field (Fig. 7A and B) [53,54]. The observed asymmetric solid state spectral line shape consisting of the weighed sum of signals from all orientations of phospholipid molecules was diagnostic of membrane lipids experiencing anisotropic motional averaging in a bilayer arrangement [52,55].

Due to non-spherical charge distribution about the phosphorous nucleus, the shielding arising primarily due to the paramagnetic contribution implies that the shielding constant depends on the orientation of the phosphate group with respect to the external magnetic field. This gives rise to ^{31}P chemical shift anisotropy (CSA) which is sensitive to both headgroup geometry and local dynamics. CSA is measured by taking the difference of chemical shift between the low field shoulder (σ_{II}) and the high-field peak ($\sigma_{\perp}$) in the proton decoupled ^{31}P NMR spectra. Residual chemical shift anisotropy ($\Delta\sigma$) observed for DSPC liposomes was in good accordance with the average ^{31}P CSA values (40–50 ppm) for lipid phosphates in extended bilayers [52,56]. The presence of co-polymer resulted in reduced CSA indicating line shape narrowing. Due to freezing of molecular motions in the viscous gel state, ^{31}P NMR spectra below the transition temperature were broad [55].

The incorporation of SMA led to further narrowing of the powder pattern at 40 °C with reduced CSA, but did not induce any significant change to the spectrum suggesting unperturbed lamellar arrangement of the phospholipid molecules. This narrowing was due to partial averaging of the $\sigma_{\perp}$ and σ_{II} components which resulted in the reduction of CSA. The amount by which CSA decreased can be related to the allowed amplitude of the motion [56].

With the increase of the temperature to 50 °C, a further narrowing in the CSA parameter of the perpendicular component indicating the onset of rapid axial rotation of phospholipids was detected for DSPC MLVs and was related to the observed pretransition in DSC studies. The SMA-induced enhanced CSA reduction signified increased mobility of the headgroup due to reorientation of the phosphate moiety. This data corroborated the DSC results, which reported decrease in the pretransition temperature.

Above the phase transition temperature (60 °C), the broad features collapsed and the powder patterns adopted a line shape characteristic of fast axially symmetric motion of the phosphate headgroup about the bilayer normal [21]. These fast lateral motions and rapid tumblings of randomly oriented phospholipid bilayers led to considerable decrease in CSA value and were due to the decrease in the correlation times of the ^{31}P headgroup motions with the transition from gel to liquid crystalline state [20]. The spectra for DSPC + SMA vesicles exhibited an additional sharp peak at 0 ppm, indicating the coexistence of anisotropic and isotropic spectral components. This was due to the presence of two distinct populations of lipid in different

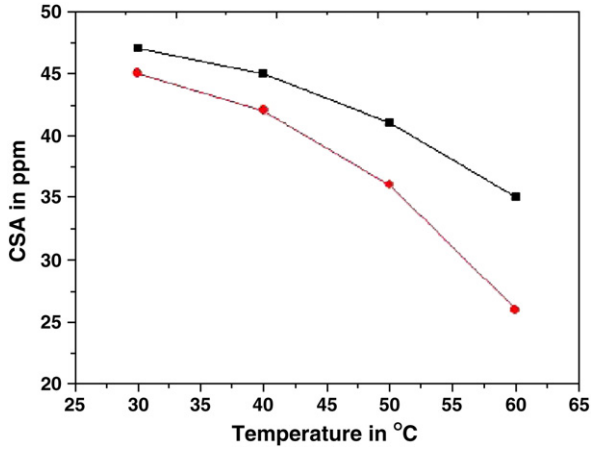

Fig. 8. Changes in chemical shift anisotropy (ppm) represented by $\Delta\sigma = \sigma_{\perp} - \sigma_{\parallel}$ for DSPC and DSPC + SMA multilamellar vesicles as a function of temperature. The black and red colors correspond to neat and co-polymer-incorporated vesicles respectively.

motional environments which were in slow exchange with one another on the ^{31}P NMR time scale. The presence of the peak at 0 ppm indicated that the membrane lipids were experiencing isotropic motional averaging either due to the formation of a small amount of unilamellar vesicles with a small size that permitted fast internal tumbling motions, or due to formation of lipid phases such as cubic or rhombic through which lateral diffusion resulted [17,56]. However, it could not be exactly determined whether there were separate populations of small and large vesicles or distinct regions of high and low curvature within the same distribution which resulted in the overlap of spectral components in presence of the co-polymer. SMA-induced enhanced reduction of the CSA (Fig. 8), suggested the existence of strong intermolecular attractions between the co-polymer and phospholipid headgroup due to the close association of the two molecules in the fluid liquid crystalline state. The presence of the isotropic spectral components indicating higher membrane fluidity [57] was consistent with the membrane fluidization detected in DSC studies and ultimately caused vesicle destabilization. Thus, the co-polymer caused significant alterations in thermotropic phase behavior, structure and organization of bilayers.

3.4.1.2. DSPC + CHOL MLVs. The presence of the co-polymer led to narrowing of the anisotropic component of the powder pattern, along with a reduced CSA for DSPC + CHOL MLVs (Fig. 9A 1 and 2) at 60 °C. Furthermore, small population of lipids was observed to undergo isotropic motional averaging (indicated by presence of a small peak at 0 ppm).

3.4.1.3. DSPC + CHOL + DODAB/DCP MLVs. The presence of the anionic co-polymer led to widening of the powder pattern of the cationic vesicles along with an increased CSA at 60 °C. Moreover, there was no evidence of any non-bilayer phases in presence of SMA (Fig. 9B3 and 4). These findings indicated decreased local mobility of the headgroup due to reorientation of the phosphate moiety in presence of SMA [17] and suggested strong electrostatic attractions, owing to increased close contacts between cationic lipids and anionic co-polymer molecules, which ultimately led to restricted axial and lateral motions of phospholipid molecules.

The spectrum obtained for the anionic vesicles at 60 °C revealed three overlapping features; two powder patterns with different CSA values, and a sharp peak at 0 ppm (Fig. 9C5). While, the broad powder pattern was characteristic of phosphatidylcholine aggregates undergoing slow reorientation, the narrow powder pattern was generated by the phosphates of DCP in the same lipid bilayers [52]. The sharp signal at 0 ppm indicated that a considerable fraction of lipids was experiencing isotropic motional averaging and might be in non-bilayer phases. The sharp spectral definition of

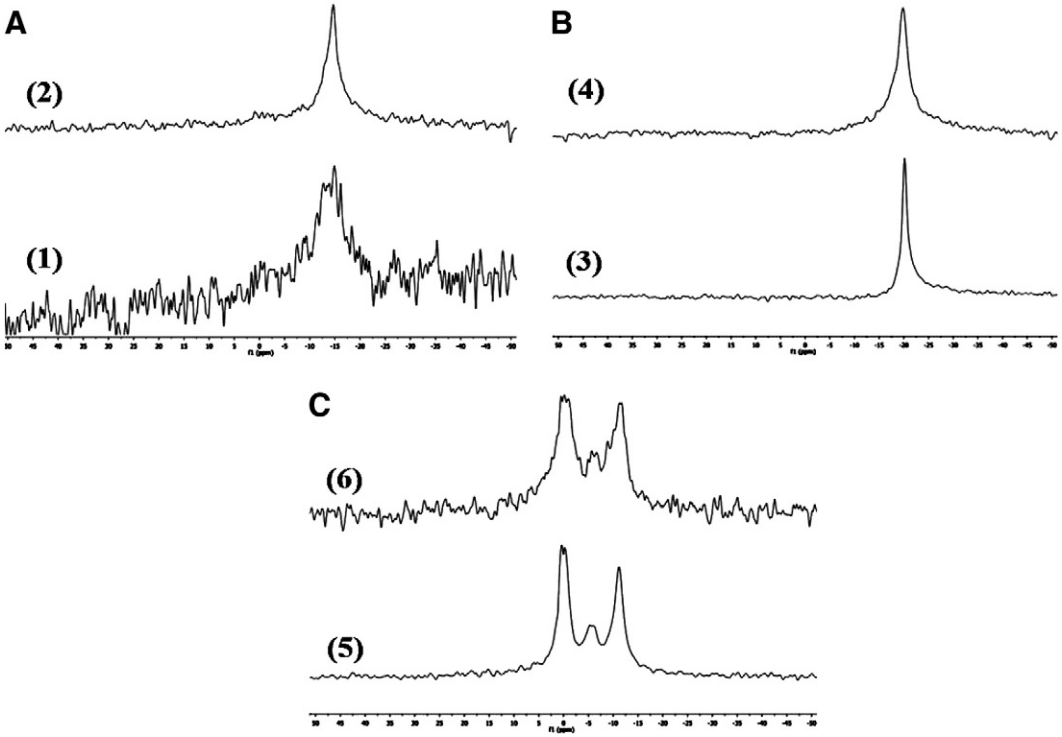

Fig. 9. 202.45 MHz ^{31}P NMR spectra of A1, DSPC + CHOL; A2, DSPC + CHOL + SMA; B3, DSPC + DODAB + CHOL; B4, DSPC + DODAB + CHOL + SMA; C5, DSPC + DCP + CHOL; C6, DSPC + DCP + CHOL + SMA MLVs at 60 °C.

the characteristic edges of the various lipid environments indicated well separated phases with none or with very slow lipid exchange between them.

Presence of the co-polymer in the anionic vesicles led to a significant increase in the intensity of the isotropic phase, and shifted both low and high field peaks of the two powder patterns (Fig. 9C6), indicating a change in the motional characteristics of the lipid environments. Moreover, the alteration of the relative intensity of the two different powder patterns with respect to each other signified a change in the DSPC/DCP ratio in the bilayers. The observed reduced spectral definition indicated an increased lipid exchange between different environments. The immensely increased population of isotropic phase with respect to anisotropic component suggested greater destabilization of the anionic membranes by the co-polymer. All these observations might be the result of significant reduction of the number of close approach contacts due to electrostatic repulsion between the negatively charged lipid headgroups and anionic SMA molecules, which led to the formation of phases undergoing fast motional averaging. This was unlike in zwitterionic PCs, where such unfavorable interactions could be balanced to an extent by maximizing contacts between the positively charged quaternary ammonium groups and negatively charged co-polymer molecules [21].

3.4.2. ^{1}H NMR spectroscopy results

Fig. 10 shows the comparison of the ^{1}H NMR spectra of SMA, DSPC and DSPC + SMA vesicles respectively. While, there was no significant change in the chemical shift of DSPC (Fig. 10D) resonances in presence of the co-polymer in the vesicles, the signals of SMA were broadened and were of diminished intensities upon incorporation into DSPC vesicles (Fig. 10E and F). These observations indicated weak immobilization of SMA within the lipid bilayers due to hydrophobic interactions between the co-polymer and lipid molecules.

4. Discussion

The observed SMA-induced alterations in the structural properties of the MLVs could be explained by considering the interactions of the co-polymer with the vesicles to occur, either through adsorption of the polymer on the lipid bilayer surface, or through the insertion of the polymer into the bilayers. Complete disruption of the bilayers into mixed polymer–lipid micelles or other aggregates could also be induced by SMA [58]. While, adsorption of the polymer would be indicated by an unaffected ΔH_{cal}, insertion or disruption of the bilayer would be associated with a decrease in ΔH_{cal} in DSC experiments. Complete disruption would however, reduce ΔH_{cal} to zero.

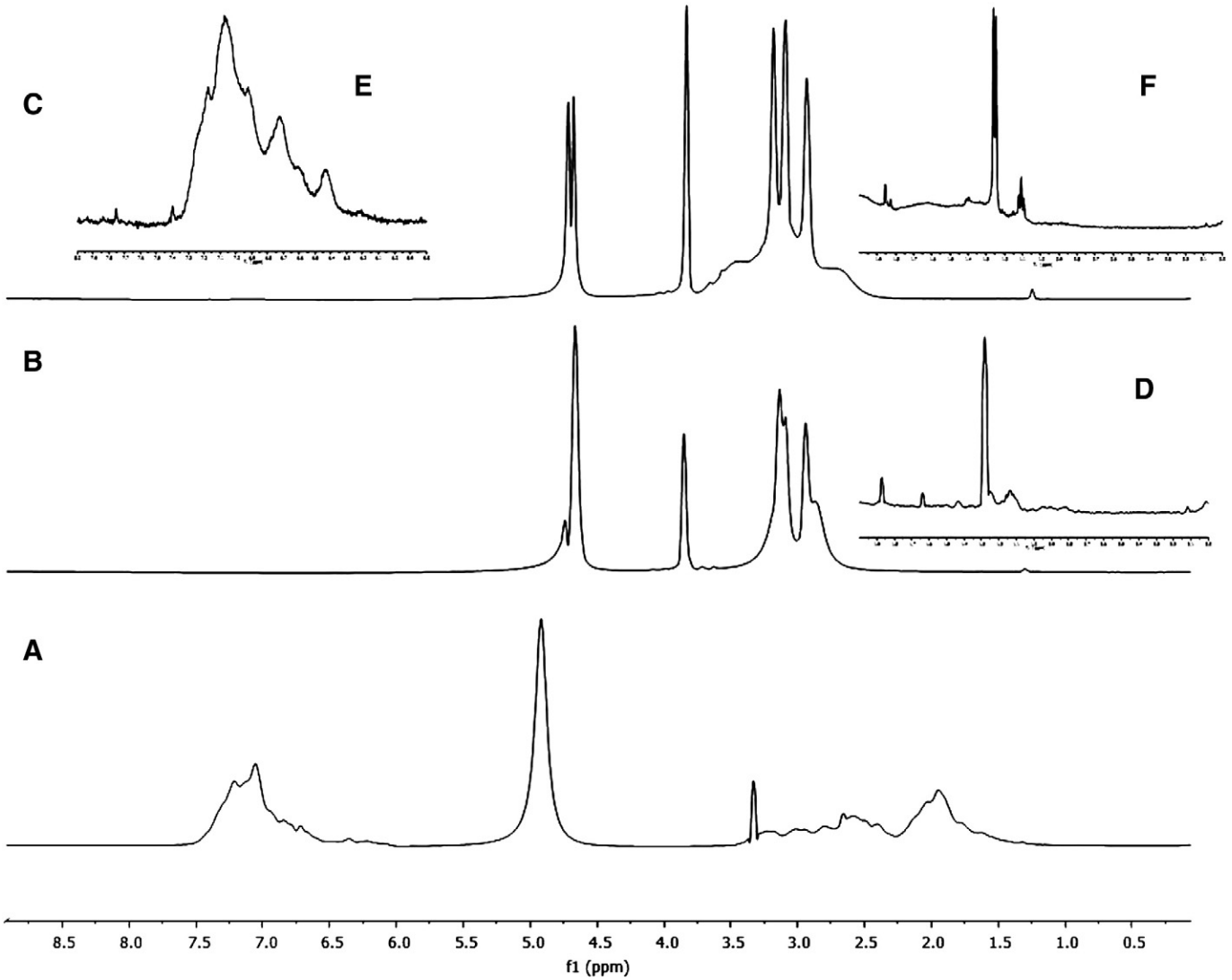

Fig. 10. 500.13 ^{1}H NMR spectra of A, SMA in deuterated methanol; B, DSPC multilamellar vesicles and C, DSPC + SMA MLVs suspended in hepes buffered saline (10 mM Hepes and 150 mM NaCl, pD 7.0) at 30 °C. Magnified views of bulk methylene and methyl proton regions (Panel D) of DSPC MLVs, aromatic proton region (Panel E) and methine, methylene and methyl proton regions (Panel F) of DSPC + SMA MLVs are also presented.

Molecular interpretation of the results obtained, indicated the role of attractive forces between SMA and zwitterionic phospholipid bilayers. The marked changes observed for pretransition in DSC experiments, the redshift of the ν_{as} and ν_s (PO_2^-) stretch frequencies in the ATR-FTIR results and the line shape narrowing detected both below and above T_m, and the existence of isotropic phases above T_m in ^{31}P NMR studies indicated increased local mobility of the phosphate groups. This was due to altered molecular packing owing to H bond formation between un-ionized carboxyl groups of the co-polymer and the phosphodiester group of phospholipids, which served as an H-bond acceptor in lipid crystals.

The weak immobilization of the co-polymer within the bilayers, appreciable reorganization of the packing of the lipid hydrocarbon portions and mild disruption of the translational order within the bilayers observed in the ^1H NMR, ATR-FTIR and DSC studies respectively, substantiated the existence of hydrophobic forces between the co-polymer and lipid molecules.

The extent of membrane fluidization and generation of isotropic phases was strongly affected by surface charge of the liposomes, and hence indicated the role of electrostatic interactions between carboxylate anions bound to the co-polymer and charged lipid headgroups. Furthermore, electrostatic interactions were also the driving force behind the observed peculiar behaviors such as charge inversion and vesiculation of membranes composed of charged lipids in the presence of SMA.

The effect of the co-polymer was evidently greater on the polar headgroup regions than on the lipid bilayer interiors of the zwitterionic phospholipid molecules. A substantial conformational change was also detected in the interfacial regions of the lipid molecules in presence of SMA. All these results suggested that SMA might be adsorbed on the bilayer surface; while a slight decrease of the thermodynamic parameters associated with the main phase transition (especially the slight decrease in ΔH_{cal}) and the immobilization of SMA within the bilayers might result from weak insertion of the hydrocarbon portions of the co-polymer probably within the interfacial region of the bilayers.

The obtained results indicating negligible destabilization of DSPC and DSPC + CHOL membranes in presence of the co-polymer were consistent with the observed cytocompatibility of SMA with murine normal fibroblastic cell line NIH/3 T3 (unpublished data). The enhanced fluidization of DSPC + CHOL + DCP membranes induced by SMA might be one of the possible reasons behind the success of RISUG as a male contraceptive, since human spermatozoa membranes have significant amount of anionic lipids. The presence of sperm breakdown products in the ejaculate of RISUG-injected subjects [59] might be due to SMA-induced destabilization of the plasma membrane and outer acrosomal membrane of human spermatozoa owing to enhanced charge repulsion. This ultimately led to vesiculation [15] and leakage of key enzymes (5′-nucleotidase and hyaluronidase) [14] that facilitate sperm-oocyte interaction. The observed complete leakage of plasma-membrane associated enzyme 5′-nucleotidase and hyaluronidase, which is specifically localized in the acrosome of human sperm, caused impairment in the gamete interactions in RISUG-injected subjects [14] and indicated effective contraceptive action of the co-polymer.

It has already been reported that anionic compounds can interact with the outer bacterial membranes through hydrogen bond and/or ionic interactions and affect membrane fluidity [60]. The significant destabilization of the MLVs composed of anionic lipids in presence of SMA leads to the speculation of probable antibacterial activity of the co-polymer via lysis of bacterial cell membranes [1] which have abundant anionic phospholipids.

With the development of DNA-loaded cationic liposomes as a non-viral gene delivery vehicle [61], the study of the interactions between polyelectrolytes and liposomes with opposite charge has started to attract attention in recent years due to its biological relevance. In spite of the recent surge in activity in this domain, lipoplexes with optimal transfection efficiency are presently unavailable [29]. Since the mechanism of interaction between polymers and oppositely charged liposomes are independent of the intrinsic structure and flexibility of the polymer [62], the characterization of SMA-loaded cationic liposomes provide valuable insights, and could be utilized in modulating the biological activity of these systems.

In conclusion, the present article reported a detailed and structured investigation on the mechanisms of interaction of SMA with model membranes and suggested a probable molecular packing model for the co-polymer within the vesicles. All the results indicated the ability of the co-polymer to reorganize the packing of the lipid molecules, which directly affected the structural integrity of model membranes. This study thus provides both, the rationale for the observed pharmacological activities of the co-polymer and the platform for future developments of SMA-based macromolecular drugs.

Acknowledgements

This work was supported by a research grant from the Ministry of Health and Family Welfare, Government of India. The authors gratefully acknowledge Prof. Rajiv Bhat of the School of Biotechnology, Jawaharlal Nehru University, New Delhi, India for kindly providing access to the VP-DSC instrument and Dr. Swapnil Gupta for her generous assistance in the DSC experiments. The authors also thank Dr. H.S. Vijayaram Kumar of MicroCal, GE Healthcare for his help in the analysis of the DSC results.

References

[1] P.K. Dhal, S.R. Holmes-Farley, C.C. Huval, T.H. Jozefiak, Polymers as drugs, Adv. Polym. Sci. 192 (2006) 9–58.
[2] B. Twaites, C.D. Alarcon, C. Alexander, Synthetic polymers as drugs and therapeutics, J. Mater. Chem. 15 (2005) 441–455.
[3] I. Donati, A. Gamini, A. Vetere, C. Campa, S. Paoletti, Synthesis, characterization, and preliminary biological study of glycoconjugates of poly(styrene-co-maleic acid), Biomacromolecules 3 (2002) 805–812.
[4] H. Maeda, SMANCS and polymer-conjugated macromolecular drugs: advantages in cancer chemotherapy, Adv. Drug Delivery Rev. 46 (2001) 169–185.
[5] A.K. Iyer, K. Greish, J. Fang, R. Murakami, H. Maeda, High-loading nanosized micelles of copoly(styrene-maleic acid)-zinc protoporphyrin for targeted delivery of a potent heme oxygenase inhibitor, Biomaterials 28 (2007) 1871–1881.
[6] S.M. Henry, M.E.H. El-Sayed, C.M. Pirie, A.S. Hoffman, P.S. Stayton, pH-responsive poly(styrene-alt-maleic anhydride) alkylamide copolymers for intracellular drug delivery, Biomacromolecules 7 (2006) 2407–2414.
[7] W.J. Fang, Y.J. Cai, X.P. Chen, R.M. Su, T. Chen, N.S. Xia, L. Li, Q.L. Yang, J.H. Han, S.F. Han, Poly(styrene-alt-maleic anhydride) derivatives as potent anti-HIV microbicide candidates, Bioorg. Med. Chem. Lett. 19 (2009) 1903–1907.
[8] V. Pirrone, S. Passic, B. Wigdahl, R.F. Rando, M. Labib, F.C. Krebs, A styrene-alt-maleic acid copolymer is an effective inhibitor of R5 and X4 human immunodeficiency virus type 1 infection, J. Biomed. Biotechnol. (2010) 1–11.
[9] H. Singh, M.S. Jabbal, A.R. Ray, P. Vasudevan, Effect of anionic polymeric hydrogels on spermatozoa motility, Biomaterials 5 (1984) 307–309.
[10] S. Banerjee, S.K. Guha, RISUG: a potential candidate for the entry inhibitor group of antiretroviral drugs, Med. Hypotheses 73 (2009) 150–152.
[11] A.M. Seddon, D. Casey, R.V. Law, A. Gee, R.H. Templer, O. Ces, Drug interactions with lipid membranes, Chem. Soc. Rev. 38 (2009) 2509–2519.
[12] T. Oda, H. Maeda, Binding to and internalization by cultured-cells of neocarzinostatin and enhancement of its actions by conjugation with lipophilic styrene-maleic acid copolymer, Cancer Res. 47 (1987) 3206–3211.
[13] S.K. Guha, RISUG (reversible inhibition of sperm under guidance) — an antimicrobial as male vas deferens implant for HIV free semen, Med. Hypotheses 65 (2005) 61–64.
[14] S.K. Guha, K. Chaudhury, A.K. Bhattacharyya, Studies on the membrane integrity of human sperm treated with a new injectable male contraceptive, Hum. Reprod. 19 (2004) 1826–1830.
[15] S.K. Guha, Contraceptive for use by a male, in: U.S. Patent No. 5488075, 1996.
[16] E. Roux, M. Lafleur, E. Lataste, P. Moreau, J.C. Leroux, On the characterization of pH-sensitive liposome/polymer complexes, Biomacromolecules 4 (2003) 240–248.
[17] K. Cieslik-Boczula, J. Szwed, A. Jaszczyszyn, K. Gasiorowski, A. Koll, Interactions of dihydrochloride fluphenazine with DPPC liposomes: ATR-IR and P-31 NMR studies, J. Phys. Chem. B 113 (2009) 15495–15502.
[18] A.B. Dhanikula, R. Panchagnula, Fluorescence anisotropy, FT-IR spectroscopy and 31-P NMR studies on the interaction of paclitaxel with lipid bilayers, Lipids 43 (2008) 569–579.
[19] F. Severcan, U. Baykal, S. Suzer, FTIR studies of vitamin E-cholesterol-DPPC membrane interactions in CH(2) region, Anal. Bioanal. Chem. 355 (1996) 415–417.

[20] H. Bensikaddour, K. Snoussi, L. Lins, F. Van Bambeke, P.M. Tulkens, R. Brasseur, E. Goormaghtigh, M.P. Mingeot-Leclercq, Interactions of ciprofloxacin with DPPC and DPPG: fluorescence anisotropy, ATR-FTIR and P-31 NMR spectroscopies and conformational analysis, Bba-Biomembranes 1778 (2008) 2535–2543.
[21] R.N.A.H. Lewis, I. Winter, M. Kriechbaum, K. Lohner, R.N. McElhaney, Studies of the structure and organization of cationic lipid bilayer membranes: calorimetric, spectroscopic, and x-ray diffraction studies of linear saturated P-O-ethyl phosphatidylcholines, Biophys. J. 80 (2001) 1329–1342.
[22] J. Grdadolnik, D. Hadzi, FT infrared and Raman investigation of saccharide-phosphatidylcholine interactions using novel structure probes, Spectrochim. Acta A Mol. Biomol. Spectrosc. 54 (1998) 1989–2000.
[23] K. Ciesik, A. Koll, J. Grdadolnik, Structural characterization of a phenolic lipid and its derivative using vibrational spectroscopy, Vib. Spectrosc. 41 (2006) 14–20.
[24] J. Grdadolnik, J. Kidric, D. Hadzi, Hydration of phosphatidylcholine reverse micelles and multilayers — an infrared spectroscopic study, Chem. Phys. Lipids 59 (1991) 57–68.
[25] S. Mansour, R.M. Hathout, N.D. Mortada, A.S. Guinedi, Liposomes as an ocular delivery system for acetazolamide: in vitro and in vivo studies, AAPS PharmSciTech 8 (2007).
[26] D.G. Fatouros, S.G. Antimisiaris, Effect of amphiphilic drugs on the stability and zeta-potential of their liposome formulations: a study with prednisolone, diazepam, and griseofulvin, J. Colloid Interface Sci. 251 (2002) 271–277.
[27] T.D. Madden, C.P.S. Tilcock, K. Wong, P.R. Cullis, Spontaneous vesiculation of large multilamellar vesicles composed of saturated phosphatidylcholine and phosphatidylglycerol mixtures, Biochemistry-Us 27 (1988) 8724–8730.
[28] C. Cametti, F. Bordi, S. Sennato, D. Viscomi, Polyion-induced liposomal vesicle aggregation: a radiowave dielectric relaxation study, J. Chem. Phys. 126 (2007).
[29] C. Cametti, F. Bordi, M. Diociaiuti, D. Gaudino, T. Gili, S. Sennato, Complexation of anionic polyelectrolytes with cationic liposomes: evidence of reentrant condensation and lipoplex formation, Langmuir 20 (2004) 5214–5222.
[30] W.R. Perkins, X.G. Li, J.L. Slater, P.A. Harmon, P.L. Ahl, S.R. Minchey, S.M. Gruner, A.S. Janoff, Solute-induced shift of phase transition temperature in Di-saturated PC liposomes: adoption of ripple phase creates osmotic stress, Bba-Biomembranes 1327 (1997) 41–51.
[31] J.S. Harris, D.E. Epps, S.R. Davio, F.J. Kezdy, Evidence for transbilayer, tail-to-tail cholesterol dimers in dipalmitoylglycerophosphocholine liposomes, Biochemistry-Us 34 (1995) 3851–3857.
[32] L. Khatri, K.M.G. Taylor, D.Q.M. Craig, K. Palin, High sensitivity differential scanning calorimetry investigation of the interaction between liposomes, lactate dehydrogenase and tyrosinase, Int. J. Pharm. 322 (2006) 113–118.
[33] M. Savva, V.P. Torchilin, L. Huang, Effect of polyvinyl pyrrolidone on the thermal phase transition of 1,2 dipalmitoyl-sn-glycero-3-phosphocholine bilayer, J. Colloid Interface Sci. 217 (1999) 160–165.
[34] B. Klajnert, R.M. Epand, PAMAM dendrimers and model membranes: differential scanning calorimetry studies, Int. J. Pharm. 305 (2005) 154–166.
[35] S. Bonora, L. Ercoli, A. Torreggiani, G. Fini, Influence of sebacate plasticizers on the thermal behaviour of dipalmitoylphosphatidylcholine liposomes, Thermochim. Acta 385 (2002) 51–61.
[36] Z. Sideratou, D. Tsiourvas, C.M. Paleos, A. Tsortos, S. Pyrpassopoulos, G. Nounesis, Interaction of phosphatidyl choline based liposomes functionalized at the interface with adenine and barbituric acid moieties, Langmuir 18 (2002) 829–835.
[37] V.V. Andrushchenko, H.J. Vogel, E.J. Prenner, Interactions of tryptophan-rich cathelicidin antimicrobial peptides with model membranes studied by differential scanning calorimetry, Bba-Biomembranes 1768 (2007) 2447–2458.
[38] L.Y. Zhao, S.S. Feng, N. Kocherginsky, I. Kostetski, DSC and EPR investigations on effects of cholesterol component on molecular interactions between paclitaxel and phospholipid within lipid bilayer membrane, Int. J. Pharm. 338 (2007) 258–266.
[39] A. Ambrosini, G. Bossi, S. Dante, B. Dubini, L. Gobbi, L. Leone, M.G.P. Bossi, G. Zolese, Lipid-drug interaction: thermodynamic and structural effects of antimicotic fluconazole on DPPC liposomes, Chem. Phys. Lipids 95 (1998) 37–47.
[40] C. Bernsdorff, R. Reszka, R. Winter, Interaction of the anticancer agent Taxol (TM) (paclitaxel) with phospholipid bilayers, J. Biomed. Mater. Res. 46 (1999) 141–149.
[41] S. Ali, S. Minchey, A. Janoff, E. Mayhew, A differential scanning calorimetry study of phosphocholines mixed with paclitaxel and its bromoacylated taxanes, Biophys. J. 78 (2000) 246–256.
[42] S.M. Gruner, R.P. Lenk, A.S. Janoff, M.J. Ostro, Novel multilayered lipid vesicles — comparison of physical characteristics of multilamellar liposomes and stable plurilamellar vesicles, Biochemistry-Us 24 (1985) 2833–2842.
[43] L.D. Mayer, M.J. Hope, P.R. Cullis, A.S. Janoff, Solute distributions and trapping efficiencies observed in freeze-thawed multilamellar vesicles, Biochim. Biophys. Acta 817 (1985) 193–196.
[44] T.P.W. Mcmullen, R.N.A.H. Lewis, R.N. Mcelhaney, Differential scanning calorimetric study of the effect of cholesterol on the thermotropic phase-behavior of a homologous series of linear saturated phosphatidylcholines, Biochemistry-Us 32 (1993) 516–522.
[45] T.P.W. Mcmullen, R.N. Mcelhaney, New aspects of the interaction of cholesterol with dipalmitoylphosphatidylcholine bilayers as revealed by high-sensitivity differential scanning calorimetry, Bba-Biomembranes 1234 (1995) 90–98.
[46] P. Martinez, A. Morros, Membrane lipid dynamics during human sperm capacitation, Front. Biosci. 1 (1996) d103–d117.
[47] S.A. Ishijima, M. Okuno, H. Mohri, Zeta potential of human X- and Y-bearing sperm, Int. J. Androl. 14 (1991) 340–347.
[48] J.G. Alvarez, B.T. Storey, Differential incorporation of fatty-acids into and peroxidative loss of fatty-acids from phospholipids of human spermatozoa, Mol. Reprod. Dev. 42 (1995) 334–346.
[49] M. Savva, V.P. Torchilin, L. Huang, Effect of grafted amphiphilic PVP-palmityl polymers on the thermotropic phase behavior of 1,2 dipalmitoyl-sn-glycero-3-phosphocholine bilayer, J. Colloid Interface Sci. 217 (1999) 166–171.
[50] T.M. Taylor, P.M. Davidson, B.D. Bruce, J. Weiss, Ultrasonic spectroscopy and differential scanning calorimetry of liposomal-encapsulated nisin, J. Agric. Food Chem. 53 (2005) 8722–8728.
[51] S. Butler, R.W. Wang, S.L. Wunder, H.Y. Cheng, C.S. Randall, Perturbing effects of carvedilol on a model membrane system: role of lipophilicity and chemical structure, Biophys. Chem. 119 (2006) 307–315.
[52] B.B. Bonev, R.J.C. Gilbert, P.W. Andrew, O. Byron, A. Watts, Structural analysis of the protein/lipid complexes associated with pore formation by the bacterial toxin pneumolysin, J. Biol. Chem. 276 (2001) 5714–5719.
[53] P.R. Cullis, A.C. Mclaughlin, Phosphorus nuclear magnetic-resonance studies of model and biological-membranes, Trends Biochem. Sci. 2 (1977) 196–199.
[54] C.M. Franzin, P.M. Macdonald, A. Polozova, F.M. Winnik, Destabilization of cationic lipid vesicles by an anionic hydrophobically modified poly(N-isopropylacrylamide) copolymer: a solid-state P-31 NMR and H-2 NMR study, Bba-Biomembranes 1415 (1998) 219–234.
[55] A. Saran, S. Srivastava, E. Coutinho, P.T.T. Wong, H. Eibl, Conformation of hexadecylphosphocholine, an anticancer drug, by molecular dynamics and NMR methods, J. Mol. Struct. 382 (1996) 23–31.
[56] C. D'Souza, M. Kanyalkar, M. Joshi, E. Coutinho, S. Srivastava, Probing molecular level interaction of oseltamivir with H5N1-NA and model membranes by molecular docking, multinuclear NMR and DSC methods, Bba-Biomembranes 1788 (2009) 484–494.
[57] O. Mertins, P.H. Schneider, A.R. Pohlmann, N.P. da Silveira, Interaction between phospholipids bilayer and chitosan in liposomes investigated by P-31 NMR spectroscopy, J. Colloid Surf. B 75 (2010) 294–299.
[58] K. Seki, D.A. Tirrell, Interactions of synthetic-polymers with cell-membranes and model membrane systems.5. Ph-dependent complexation of poly(acrylic acid) derivatives with phospholipid vesicle membranes, Macromolecules 17 (1984) 1692–1698.
[59] V. Koul, A. Srivastav, S.K. Guha, Reversibility with sodium bicarbonate of styrene maleic anhydride, an intravasal injectable contraceptive, in male rats, Contraception 58 (1998) 227–231.
[60] P.M. Furneri, M. Fresta, G. Puglisi, G. Tempera, Ofloxacin-loaded liposomes: in vitro activity and drug accumulation in bacteria, Antimicrob. Agents Chemother. 44 (2000) 2458–2464.
[61] V.P. Torchilin, Recent advances with liposomes as pharmaceutical carriers, Nat. Rev. Drug Discov. 4 (2005) 145–160.
[62] E. Raspaud, M.O. de la Cruz, J.L. Sikorav, F. Livolant, Precipitation of DNA by polyamines: a polyelectrolyte behavior, Biophys. J. 74 (1998) 381–393.